Shearing of Polymer Drops with Interface Modification

Leon Levitt[†] and Christopher W. Macosko*

Department of Chemical Engineering and Materials Science, University of Minnesota, Minneapolis, Minnesota 55455

Received September 22, 1998; Revised Manuscript Received May 24, 1999

ABSTRACT: The influence of block copolymers (BCP) and interfacial reaction on the deformation of 30−100 μm polymer drops inside an immiscible polymer matrix was visualized in a parallel plate, counterrotating apparatus. Symmetric diblock copolymers were blended into polypropylene (PP), poly(methyl methacrylate) (PMMA), and polyethylene (PE) homopolymers. These were dispersed as drops in a polystyrene (PS) matrix. Addition of BCP significantly increased the amount of area the deforming drop generates when subjected to simple shear flow. Polymers with terminal amine groups (PMMA and PS) were coupled with maleic anhydride functional PS and PE. This reaction results in the formation of graft copolymer at the interface. These reactive pairs appear to be even more effective than BCP at generating interfacial area. The enhancement in area may be attributed to reduction in interfacial tension or to reduction in slip, but more likely a combination of both and a gradient in interfacial tension.

Introduction

Drop deformation is important for understanding how the morphology develops in immiscible polymer blends. For example, if drops of an impermeable minor phase are stretched into sheets or platelets, barrier properties of the matrix can be improved dramatically.[1] In this paper we observe molten polymer drops as they are sheared within an immiscible matrix. In previous visualizations viscosity was low enough that interfacial tension caused the deformed drops to maintain approximately a circular cross-section.[2−4] Previous analyses have used this observation to assume symmetry and thus reduce computation to a two-dimensional problem.[2,4−6] The viscosity of molten polymers is so high, typically >1000 Pa·s, that interfacial tension has little effect on the initial shear deformation of drops with 50 μm or greater diameter. Such drops deform to an ellipsoid (see Figure 1) affinely with the matrix, i.e., the length increasing proportional to strain and the width remaining constant. We have even observed width to *increase* due to normal stresses in the matrix.[7]

However, at large deformation, curvatures become very high and interfacial forces win out. Width begins to contract, and the length stops increasing. Edges may even pinch off or the drop break up via Rayleigh-type instability. To create polymer blends with a high diffusion barrier, we want the drops to deform into very long and wide platelets. The goal is to significiantly increase the cross-sectional area of the minor phase in the plane of shearing. Adding block or graft copolymers to the minor phase should reduce interfacial tension and interfacial slip. The goal of this study is to test the effectiveness of this strategy. We have used both premade diblock copolymers and graft copolymers created by reaction across the interface. Their effectiveness was measured in terms of area generation during shear visualization.

Experimental Section

Pairs with Block Copolymers. The list of materials used with premade block copolymers is given in Table 1. Viscoelastic properties, η^* and G' measured with 25 mm parallel plates in a Rheometrics RMS at 1 rad/s and 200 °C, are also given. Two polypropylenes with melt indices 2 and 30 (PP2 and PP30) were obtained from Huntsman Chemical Co. Polystyrene (PS) homopolymer, Styron 666D, and high-density polyethylene (PE) were provided by Dow Chemical Co. Poly(methyl methacrylate), PMMA, is from Rohm & Haas.

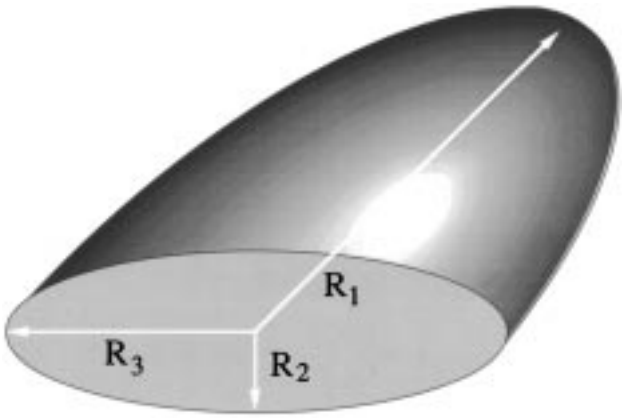

Figure 1. Schematic drawing of a stretching drop. The drop is approximated as an ellipsoid with three radii: R_1, R_2, and R_3.

All three block copolymers (BCP) had one PS block and were synthesized at the University of Minnesota. P(S-*b*-EE) is a symmetric copolymer (50 wt % polystyrene) with one block containing, randomly, 70% ethyl ethylene (hydrogenated 1,2-butadiene) and 30% ethylene (hydrogenated 1,4-butadiene), and the other block was PS. Both blocks have molecular weight of 50 000, with narrow molecular weight distribution: $M_w/M_n = 1.05$.[8] Bates et al. have shown that the EE block of this BCP is miscible in polypropylene.[8] The other two copolymers were P(S-*b*-MMA)[9] with M_w = 85 000, and P(S-*b*-E) with M_w = 40 000.[10] Both BCPs were also symmetric with narrow molecular weight distributions. Each BCP was first mixed at 10% into a homopolymer, as shown in Table 1, and then used to form drops in the PS matrix, as indicated in Table 2.

For the block copolymer to provide effective coupling between the phases each block should be longer than the molecular weight between entanglements, M_e.[11] Fetters et al.[12] report M_e for PS is 13 000. M_e for PEE is 11 000, for PMMA is 4700, and for PE is 1250.[12−14] Thus all the blocks exceed M_e.

Reactive Pairs. The list of reactive polymers and their rheological properties is given in Table 3. Three nonreactive

* To whom correspondence should be addressed.
[†] Current address: 3M Center/CRPTL, 208-1, St. Paul, MN 55144.

10.1021/ma9814999 CCC: $18.00
Published on Web 09/01/1999

Table 1. Properties of Homopolymers, Block Copolymers, and Their Blends at 200 °C

polymer (abbreviation)	M_w (supplier)	η^*, Pa·s $\omega = 1\ s^{-1}$	G', Pa $\omega = 1\ s^{-1}$	Γ, mN/n with PS
	Homopolymers			
poly(methyl methacrylate) (PMMA)	110 000 (Rohm & Haas)	43 000	16 800	1.5[22,28] 0.8[25]
polyethylene (PE)	160 000 (Dow Chemical)	1 610	273	4.7[25,26] 4.9[33]
polystyrene (PS)	100 000 (Dow Chemical)	4 940 1 070[a]	1730 185[a]	–
polypropylene, melt index 2 (PP2)	~100 000 (Huntsman)	4 720[a]	220[a]	4.5[25,27] 5.0[28]
polypropylene, melt index 30 (PP30)	~50 000 (Huntsman)	854	121	
	Block Copolymers			
P(S-*b*-EE)	100 000 (ref 8)			
P(S-*b*-MMA)	85 000 (ref 9)			
P(S-*b*-E)	40 000 (ref 10)			
	Blends (10% BCP)			
PMMA + P(S-*b*-MMA)		30 500	12 600	
PE + P(S-*b*-E)		1 630	320	
PP2 + P(S-*b*-EE)		3 000[a]	850[a]	
PP30 + P(S-*b*-EE)		545	67	

[a] Measured at 220 °C.

Table 2. Drops with and without Block Copolymer in PS Matrix

drop	initial diam, μm	η_r	G'_r	$\dot{\gamma}$, s^{-1}	A_r^{max}	γ^{max}	R_2,[a] μm
PP30	90	0.2	0.07	0.9	4	6	11
PP30 + P(S-*b*-EE)	95	0.1	0.04	1.1	18	22	2.6
PP2	120	4.4	11.9	0.9	4	9	15
PP2 + P(S-*b*-EE)	110	2.8	4.6	1.15	9	16	6
PMMA	60	8.7	9.7	0.95	4	8	7.5
PMMA + P(S-*b*-MMA)	32	6.2	7.3	1.0	6.5	11	2.5
PE	65	0.3	0.2	1.2	5	9	6.5
PE + P(S-*b*-E)	55	0.3	0.2	1.4	8	17	3.4

[a] R_2 (drop thickness/2) at γ^{max}.

Table 3. Properties of Reactive Polymers at 220 °C

polymer (abbreviation); trade name	M_w (supplier)	η^*, Pa·s $\omega = 1\ s^{-1}$	G', Pa $\omega = 1\ s^{-1}$	reactivity
polyethylene (PE-MA); Polybond	110 000 (Uniroyal)	1900	570	4.5% maleic anhydride (graft)
polypropylene (PP-MA)	30 000 (Elf Atochem)	110	80	1% maleic anhydride (graft)
poly(methyl methacrylate) (PMMA27)	27 000 (ref 9)	4500	350	nonreactive
poly(methyl methacrylate) (PMMA-NH_2)	29 000 (Polymer Source)	3400	270	aliphatic amine (end functional)
polystyrene (PS23)	23 000 (ref 15)	45	30	nonreactive
polystyrene (PS-NH_2)	23 000 (ref 15)	100	110	amine (end functional)
polystyrene (PS-OX); RPS	~100 000 (Dow)	1450	260	1% oxazoline (random copolymer)
polystyrene (PS-MA); Dylark	~100 000 (Arco)	1600	250	5% maleic anhydride (random copolymer)

polymers were also used in the study. Poly(methyl methacrylate), PMMA27, with $M_w = 27\ 000$ was prepared by means of anionic polymerization.[9] Polystyrene, PS23, with $M_w = 23\ 000$ was prepared by living radical polymerization and provided by DeSimone and co-workers.[15] The polypropylene is PP30; see Table 1. Reactive materials include polymers with amine, maleic anhydride, or oxazoline groups. Aliphatic amine terminated poly(methyl methacrylate), PMMA-NH_2, was obtained from Polymer Source Co. (Montreal). The polymer has $M_w = 29\ 000$ and a polydispersity, M_w/M_n, of 1.05, as expected for anionic polymerization. Ninety-four percent of the chains are terminated with an amine group. The other amine-functional polymer was polystyrene (PS-NH_2) with $M_w = 23\ 000$ and a polydispersity of 1.16.[15] Both PMMA-NH_2 and PS-NH_2 have an aliphatic amine terminal group which is very reactive toward anhydride.[16]

All three polymers with maleic anhydride (MA) have multiple functionality with various contents of MA. Polybond (PE-MA), a low density polyethylene, with grafted MA groups was obtained from Elf Atochem and has functionality of 4.5 wt %. Low molecular weight polypropylene (PP-MA) is also a graft copolymer from Elf Atochem and has about 1 wt % MA groups. The PS-MA is a random copolymer (Dylark, Arco Chemical) which contains 5 wt % MA. PS-OX is 1 wt % oxazoline functional polystyrene copolymer obtained from Dow Chemical. Polymer pairs are listed in Table 4. As mentioned earlier, all reactions are imidation type between amine and MA, except the last pair. In the reaction between PP-MA and PS-OX, oxazoline undergoes a ring opening reaction with maleic anhydride.[17,18] Due to multiple functionality of both polymers the reaction leads to cross-linking at the interface.

Sample Preparation. About 10 wt % of a block copolymer was blended into each homopolymer using a miniature cup mixer (CSI Co. Sterling Heights, NJ) described in detail by Sundararaj et al.[19] About 50 mg of BCP powder was added to 0.5 g of homopolymer and then mixed at 200 °C for 10 min. To improve distributive mixing, the rotor was lifted every minute. After blending, a thin fiber was drawn from the corner of the cup, where the highest shear rate, and thus best mixing, is expected.

Thin fibers of the polymer selected to be the droplet phase were prepared by drawing the melt from a heated stage (Mettler, FP80 HT). The temperature of the hot stage was controlled at 200 °C. The matrix was prepared in the form of 31 mm diameter, 1 mm thick disks using a heated press. The fibers were placed in the visualization apparatus between two

Table 4. Drops with and without Terminal Reactive Groups, Area Generation at 220 °C, and Actual Shear Rate

drop	matrix	initial diam, μm	η_r	G'_r	$\dot{\gamma}$, s^{-1}	A_r^{max}	γ^{max}	R_2,[a] μm
		87				14	20	3
PS23	PE-MA	67	0.02	0.05	2.1	10	18	3.3
		40				7.5	12	2.7
		59				24	50	1.2
PS-NH2	PE-MA	40	0.05	0.2	2.3	13	24	1.5
		31				8	10	1.4
PMMA27	PS-MA	80	2.8	1.4	0.9	8	≈30	5
PMMA-NH_2	PS-MA	70	2.1	1.1	1.05	>35	>40	<1
PP30	PS-OX	82	0.6	0.5	0.95	13	17	3
PP-MA	PS-OX	irregular	0.08	0.3	1	undeformed		

[a] R_2 (drop thickness/2) at γ^{max}.

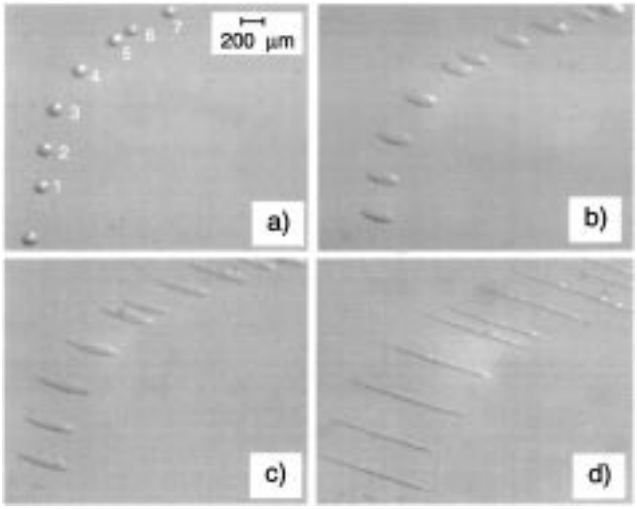

Figure 2. PE drops in PS matrix ($Ca = 50$, $\eta_r = 0.3$, $G'_r = 0.2$). (a) The fiber that broke up into drops was slightly bent. Drops differ in size from 84 to 112 μm. (b) $\gamma = 3$. No change of the drop width is observed. (c) At $\gamma = 6$ interfacial tension starts prevailing, and the "pancakes" become narrower. (d) At $\gamma = 20$, the drops become fibers.

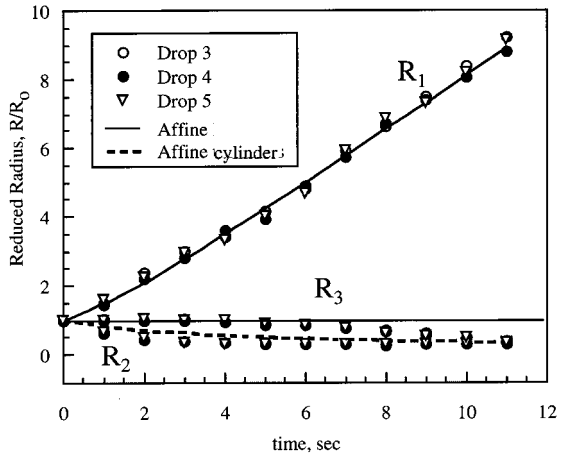

Figure 3. Reduced length, width, and thickness plotted vs shear strain for three PE drops, drops 3−5, from Figure 2. Although the drops differ slightly in size, they deform affinely in R_1. From the deformation the shear rate is determined; $\dot{\gamma} = 0.9$ s^{-1}. The width, R_3, deviates from affine at $\gamma > 5$, and the drop becomes cylindrical by $\gamma = 11$. The thickness, R_2, was not measured but calculated from R_1 and R_3.

matrix disks and heated to 200 °C for about 1 h. Interfacial tension caused the fiber to break into a string of droplets, as shown in Figure 2a. Drops are typically ~100 μm in diameter and thus 20 drop radii away from the plates. Wall effects are expected to become negligible above 5 radii away. Further details of the procedure are provided by Levitt.[7,20]

Visualization. Visualization was done between heated, counterrotating glass disks. Temperature can be controlled to ±2 °C. Drop dimensions are measured to ±1 μm using a high-magnification, long focal length lens and CCD camera. The device is described in detail elsewhere.[7,20]

We obtained the effective shear rate by tracking the length change of the drops with time. Figure 2 illustrates several PE drops sheared in a PS matrix. The shape of the drop can be approximated by an ellipsoid with three radii R_1, R_2, and R_3, as illustrated in Figure 1. Figure 3 shows the reduced radii vs time of three drops of about same initial size (~90 μm) from Figure 2. If the width remains constant and the drop elongates with the flow (affine deformation), the length ($2R_1$) follows:[21]

$$\text{affine} \qquad R_1 = R_0\left[1 + \frac{\gamma^2}{2} + \frac{\gamma}{2}[4 + \gamma^2]^{1/2}\right]^{1/2} \tag{1}$$

$$R_2 = R_0\left[1 + \frac{\gamma^2}{2} - \frac{\gamma}{2}[4 + \gamma^2]^{1/2}\right]^{1/2} \qquad R_3 = R_0$$

where γ is the shear strain and R_0 the initial drop radius. Figure 3 shows that for all three drops R_1 deforms affinely up to strains of 10. Shear rate calculated from the fit of R_1 vs time data to eq 1 was within 5% of the value calculated from the speed of the glass disks, matrix thickness, and radial location of the drop. Shear rates in all these experiments are about 1 s^{-1}.

Although in Figure 3 the drop length follows eq 1, the width begins to decrease at $\gamma = 5$ and by $\gamma = 11$ the drop is an ellipsoid of revolution, i.e., nearly cylindrical, $R_2 = R_3$. For affine deformation of an ellipsoid of revolution, R_1 follows eq 1, while from mass conservation R_2 and R_3 decrease according to[21]

$$\text{affine cylinder} \qquad R_2 = R_3 = R_0\left[1 + \frac{\gamma^2}{2} + \frac{\gamma}{2}[4 + \gamma^2]^{1/2}\right]^{-1/4} \tag{2}$$

In some cases affine deformation was not observed for short times, $t < 1$ s. Drops deformed very little, although they moved across the video screen. This is due to backlash in the fork holding the upper quartz disk and in the gears of the rotary stage driving the lower disk.[7,20]

The efficiency of stretching was measured using the reduced area parameter, A_r, which is the ratio of the projected area of the deforming drop to the projected area of the initial drop, πR_0^2. The projected area of the drop was approximated as an ellipse, with an area $A = \pi R_1 R_3$.

The elliptical fit of the area may overestimate the real value, since the ends of the platelets are more pointed at large values of strain, as shown in Figure 2d and Figure 4c for the PP30/PS pair. In Figure 4c, a thick edge bead due to the effect of interfacial tension is also visible. At even larger strain, the thin film between the edges ruptures and the platelet becomes doughnut-like.[22]

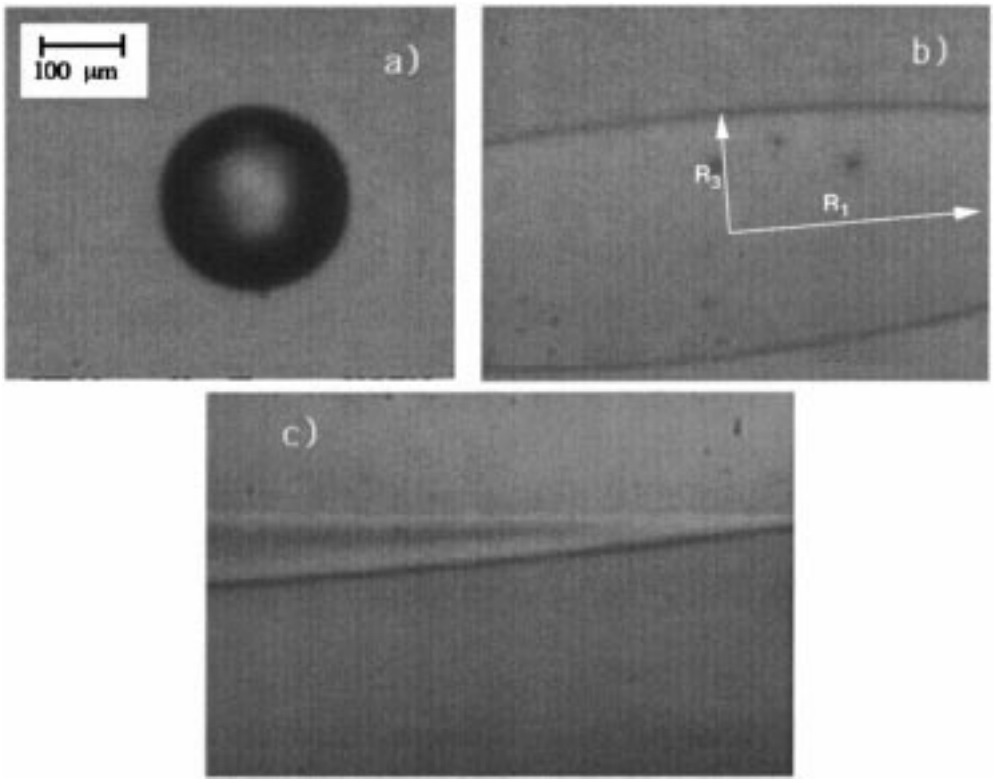

Figure 4. Edge bead in the PP30/PS pair. (a) This is an undeformed drop. (b) About 25% widening is observed at $\gamma \approx 10$. (c) At a higher value of strain the ends of the drops become pointed, and the edges thicken due to the effects of interfacial tension.

Another possible source of error in the estimate of the projected area is drop tilt. For affine deformation the angle θ between the R_1 drop axis and the flow direction decreases with strain[21]

$$\tan\theta = ({}^1/_2\gamma + {}^1/_2[4+\gamma^2]^{1/2})^{-1} \quad (3)$$

For a strain of 2 the tilt is 23° and the projected area is just 8% smaller than the true area, $\pi R_1 R_3$. Thus the projection error was ignored.

Results

In drop deformation studies the capillary number, the ratio of shear stress to interfacial stress, is often used[2]

$$Ca = \eta\dot{\gamma}R/\Gamma \quad (4)$$

where Γ is the interfacial tension. For most drop deformation visualizations in the literature $Ca \leq 1$; i.e., interfacial stresses are large. Drops deform moderately and reach an equilibrium shape quickly. For example, Guido and Villone[23] recently showed shear deformation of 50 μm diameter. PDMS drops in a poly(isobutylene) matrix with $\eta = 81$ Pa·s. The shear rate was low, giving $Ca = 0.2$, and steady-state deformation was reached at $R_1/R_0 < 2$. Polymer melts are much more viscous and, as Figure 3 indicates, deform extensively. In this work $Ca \cong 50$. In some processing flows equilibrium shapes may never be achieved; for barrier films they are undesireable.

Materials with Block Copolymers. P(S-*b*-EE) added to PP2 made a significant difference in the way the polypropylene drop deformed. Parts a−c of Figure 5 show an uncompatibilized PP2 drop in PS ($\eta_r = 4.4$, $G'_r = 11.9$) matrix at strains $\gamma = 0$, 3, 20. G'_r represents the drop/matrix elasticity ratio, G'_d/G'_m. The drop deforms like a pointed cylinder. Addition of BCP reduces

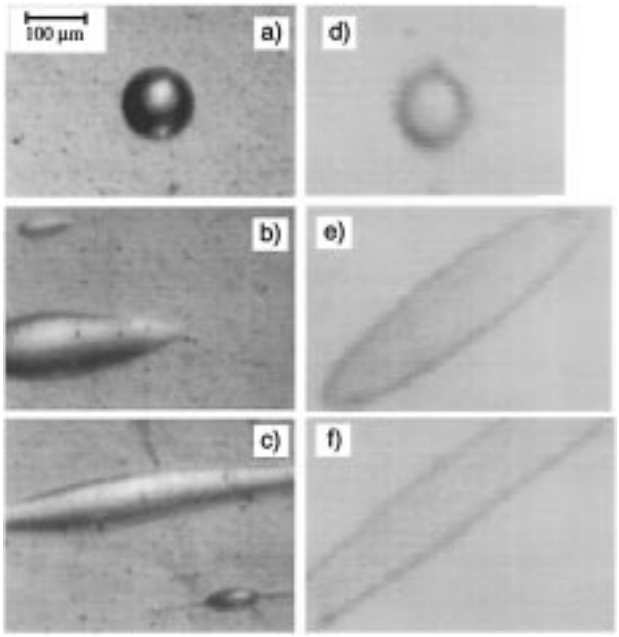

Figure 5. Micrograph of PP2 drop without BCP and with P(S-*b*-EE) in PS matrix at 220 °C. (a) This is a noncompatibilized drop at $\gamma = 0$. (b) The drop forms a torpedo-like shape when $\gamma = 3$. (c) $\gamma = 20$. (d) This is an undisturbed PP2 drop with 10% P(S-*b*-EE) BCP. (e) A flat shape is formed at $\gamma = 6$. (f) even at $\gamma \sim 12$ the sheetlike geometry is maintained.

interfacial tension but also surprisingly the viscosity (see Tables 1 and 2).[24] A significant increase in projected area is observed. The width of the platelet in Figure 5f is equal to the diameter of the drop even at $\gamma = 20$.

In our previous work, it was shown that a more elastic matrix causes less elastic drops to widen in the vorticity direction, i.e., perpendicular to the direction of flow due to the second normal stress of the matrix.[7] PP30/PS

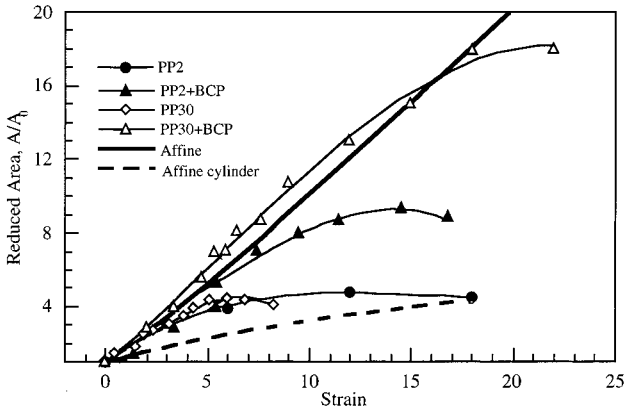

Figure 6. Influence of BCP on the reduced area generation for P2 and PP30 drops in PS matrix. PP2 without BCP follows the affine cylinder deformation. Addition of BCP doubles A_r at $\gamma = 15$. PP30 drop ($\eta_r = 0.2$, $G'_r = 0.07$) starts as affine but quickly declines due to interfacial tension, $\Gamma = 5$ mN/m. The PP30/P(S-*b*-EE) ($\eta_r = 0.1$, $G'_r = 0.04$) drop generates an area larger than affine due to widening caused by matrix normal stresses.[7] There is more than a 4-fold increase in the area.

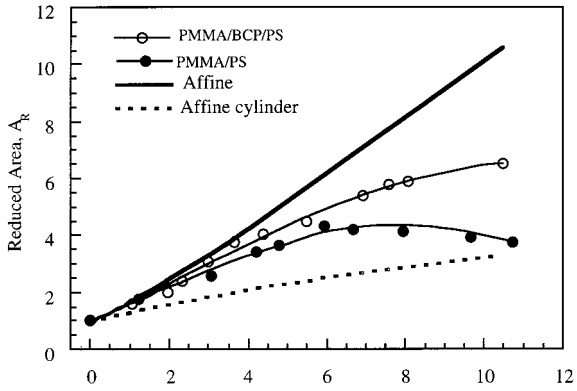

Figure 7. Reduced area for PMMA drops in PS matrix ($\eta_r = 8.7$, $G'_r = 9.7$, $D_0 = 60$ μm) with 10% P(S-*b*-MMA) BCP ($\eta_r = 6.2$, $G'_r = 7.3$, $D_0 = 32$ μm). Although a noncompatibilized drop is twice as big as the PMMA drop with P(S-*b*-MMA) BCP, it generates less area.

represents such a case; $G'_r = 0.1$ indicates that the matrix has much higher normal stresses. As a result the width of the drop increases (see Figure 4b), until the stress from interfacial tension becomes equal to the difference in normal stresses between the two phases.

Figure 6 illustrates area generation for PP2 and PP30 drops sheared in the PS matrix with and without P(S-*b*-EE) copolymer. The graphs are compared to affine (eq 1) and affine cylinder (eq 2) deformations. The effect of BCP is quite evident. The maximum reduced projected area for PP2 without compatibilizer is 4. Addition of 10% P(S-*b*-EE) more than doubles A_r^{max}. The lower viscosity PP30 with 10% of the same BCP produces an even bigger effect when sheared in the same matrix. There is a quadruple increase in the reduced area over the noncompatibilized PP30/PS666. Widening of the compatibilized PP30 drop results in more than affine area generation.

Figure 7 shows results for PMMA drops in a PS matrix. The drops are much more viscous and elastic than the PS matrix: $\eta_r = 8.7$, $G'_r = 9.7$ for the PMMA/PS system, and $\eta_r = 6.2$, $G'_r = 7.3$ for the PMMA + P(S-*b*-MMA)/PS pair. Thus, we do not expect any widening, and affine deformation is the limit for A_r. Figure 7 and Table 2 show that when the diblock copolymer was

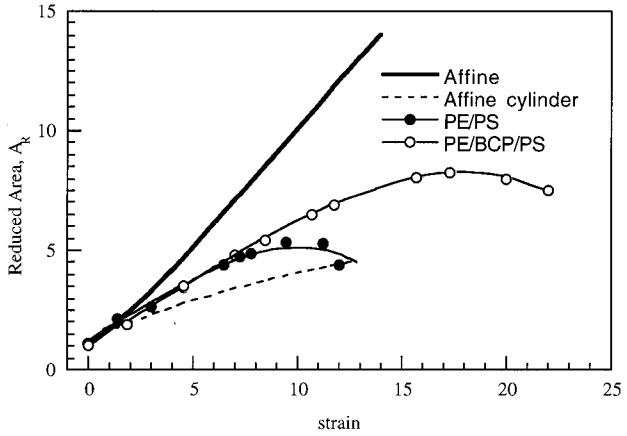

Figure 8. Shear of PE drops in PS matrix with and without P(S-*b*-E) copolymer ($\eta_r = 0.3$, $G'_r = 0.2$). $D_0 = 55$ μm with and 65 μm without.

added to PMMA, A_r increased more than 50% despite the fact that the initial drop was much smaller. It should be noted that, according to the analysis of Van Oene,[29] the drop should not be deforming at all. Van Oene argued that the difference in normal stresses between the drop and the matrix should be added to the stress from interfacial tension. We calculated the normal stress assuming the shear rate inside the drop is the same as the matrix. The normal stress plus interfacial stress is significantly bigger than the shear stress exerted by the matrix, yet the drops deform. Also several studies on Newtonian drops have shown that for $\eta_r \geq 4$ the drops should reach a stable shape and stop deforming.[2−4] Both the compatibilized and noncompatibilized PMMA drops exceed this critical ratio.

The area generation results in Figure 8 for PE drops in PS, and those of PE + P(S-*b*-E)/PS are similar to the PMMA results. A_r for the drops with P(S-*b*-E) generated 60% more area than the uncompatibilized drop, when compared at A_r^{max}.

The values of R_2 in Table 2 are at the strain causing maximum area generation. They illustrate the efficiency of area generation from a different perspective. The value of R_2, which represents the thickness of the drops, is always smaller for the compatibilized pairs. If the drops are simple ellipses, then $1/R_2$ is the maximum curvature where the maximum interfacial stress is generated. At this point interfacial stresses are stopping further area growth. If we put these values into eq 4 along with $\dot{\gamma}$ and PS viscosity and interfacial tension values from Table 1, we calculate a capillary number of roughly 10. If we assume that, at about this same value of the capillary number, area generation should reach a maximum for the drops with added block copolymer, then the ratios of R_2 in Table 2 are a measure of the decrease in interfacial tension. These ratios suggest that block copolymer decreases Γ by a factor of 2−3 in all five pairs. Such reductions for 10% block copolymer have been observed.[26]

Reactive Pairs. A very significant improvement in area generation was found for the reactive PMMA-NH_2/PS-MA pair over nonreactive PMMA/PS-MA. The effect is shown in Figure 9. In both cases the drop is more viscous than the matrix ($\eta_r = 2.8$ for nonreactive and 2.1 for reactive). The width of the stretched reactive drops almost does not change for the duration of the experiment ($\gamma = 40$), when the sheet of PMMA-NH_2 became so thin that we could no longer observe it. The

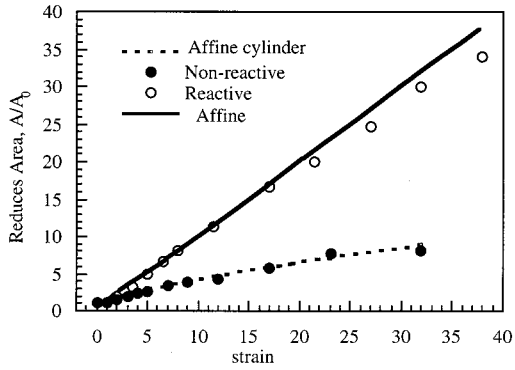

Figure 9. Reduced area vs strain for the reactive and nonreactive PMMA in PS-MA matrix.

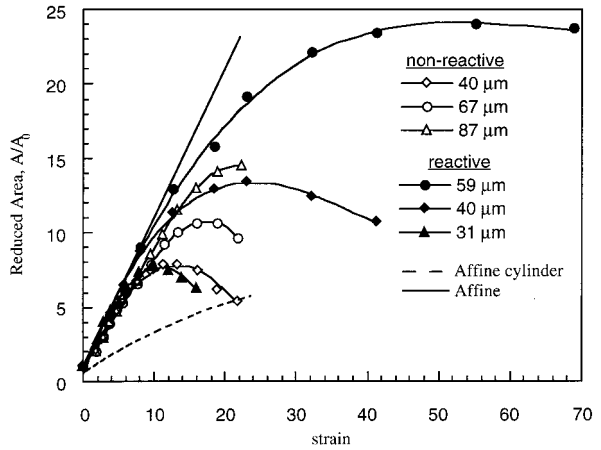

Figure 10. Reduced area plotted versus strain for nonreactive PS23/PE-MA (open symbols) and reactive PS-NH2/PE-MA (solid symbols) pairs. As expected, all drops fall on the same curve at low strain. Reaction at the interface delays the maximum for A_r and results in larger interfacial area.

reduced area is slightly smaller than affine but follows the trend to very high strains, as seen in Figure 9. At $\gamma = 30$, there is more than a 4-fold increase in A_r over the nonreactive case. The difference should increase even more with strain.

Reduced area is plotted in Figure 10 for three nonreactive drops of PS23 with diameters 40, 67, and 87 μm sheared in PE-MA. These low-viscosity drops ($\eta_r = 0.02$) at small strain, $\gamma < 7$, follow affine deformation, and the values of the reduced area are the same for all three. The difference in shear rate between the drops due to the difference in radial position in the parallel plates does not exceed 2%. Using the method described in Figures 2 and 3, the shear rate was estimated to be 2.1 s^{-1}. The maximum in area generation was observed at $\gamma = 12$ for a 40 μm drop and $\gamma = 20$ for 87 μm drop, increasing with drop size as expected.

In the experiment with reactive PS-NH_2/PE-MA we also observed three drops. Two of them, 40 and 59 μm, are similar in size to the nonreactive ones. The diameters are close, and shear rate was found to be similar, 2.3 s^{-1}. The maximum for a 40 μm reactive drop was significantly delayed from 12 to 24 strain units. A more remarkable improvement was observed for the 59 μm drop—no decline of A_r until $\gamma \cong 50$.

Table 4 summarizes the more efficient area generation of the reactive drops. The thickness of the PS-NH_2 drop (represented by R_2) is about half of the nonreactive one. This indicates that the reactively formed graft copolymer between PS and PE has halved their interfacial tension, using the same argument given above with respect to R_2 for block copolymer modified drops. For the PMMA-NH_2 drop in the PS-MA matrix, R_2 for the reactive and nonreactive pairs indicate Γ is reduced by a factor of 5. Such a large decrease in interfacial tension is about the maximum that has been attributed to block copolymers in the literature.[26,30,31]

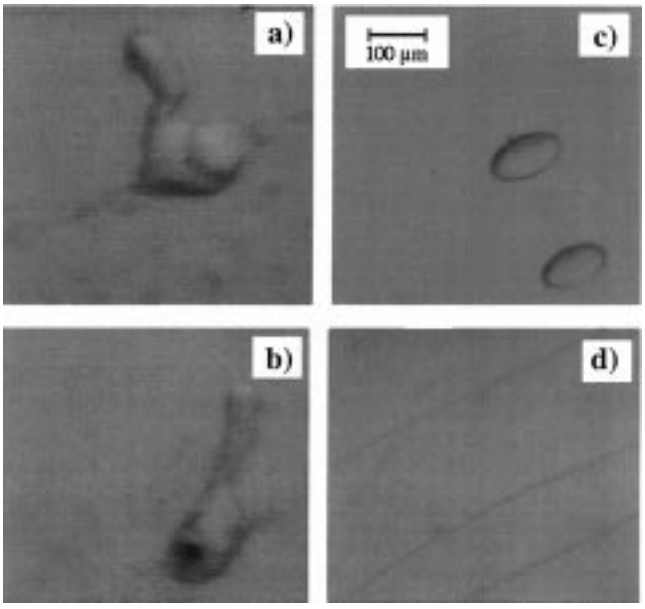

Figure 11. Cross-linking reaction between PP-MA drop and PS-OX matrix makes the interface less mobile. As a result no deformation was observed despite low rheological ratios ($\eta_r = 0.08$, $G'_r = 0.3$) at $\dot{\gamma} = 1$ s^{-1}, as shown in (a) $\gamma = 0$ and (b) $\gamma = 15$. The irregular shape of the drop is due to the difficulty in breaking the fiber. Micrographs (c) $\gamma = 1$ and (d) 15 represent the nonreactive PP30/PS-OX case. The drop stretches into a sheet.

Note in Table 4 that regardless of their initial diameter all the nonreactive drops have about the same thickness at the maximum in area generation $R_2^* = 3-5$ μm. The same is true for the reactive drops except R_2^* is smaller ($\cong 1$ μm). This is similar to the results in Table 2 and is another argument for a critical value of Ca at maximum area generation, although here $Ca^* \cong 3$ for nonreaction drops compared to roughly 10 for the uncompatibilized polymers in Table 2. Clearly a more complete analysis of drop deformation would be helpful. Viscosity ratio and elasticity must also be important. Elasticity may cause drops at large deformation to not be ellipsoidal, e.g., Figures 4c and 5b,c. We are currently pursuing a full finite element aided analysis of viscoelastic drop deformation.[32]

The last reactive pair in Table 4 can cross-link due to multiple fundamental groups on both polymers. Cross-linking has a dramatic effect on the drop/matrix interface. The PP-MA fiber was very stable after 5 h of heating inside the PS-OX matrix at 220 °C. Only after the fiber was sheared in both directions did it break into objects, and these never assumed spherical shape. Further shearing at $\dot{\gamma} = 1$ s^{-1} had no effect on drop deformation, as shown in Figure 11a,b. Nonreactive PP30, on the contrary formed sheets, as shown in Figure 11c,d.

Interfacial Tension Reduction, Slip, or Tension Gradient?

Another explanation for the increase in area generation when block copolymers are added or formed by

interfacial reaction is that, in addition to decreasing interfacial tension, the copolymers increase adhesion. De Gennes[33] and also Goveas and Fredrickson[34] have pointed out that there must be a reduction in entanglements close to the interface between two immiscible polymers. This leads to much lower viscosity or a slip layer in the interface. Block or graft copolymers can span the interface and eliminate the slip layer.[33] The PS-*g*-PMMA and PE-*g*-PS copolymers formed at the interfaces of our drops (Figures 9 and 10) may be of very high molecular weight with many entanglements across the interface.[20,40]

In principle it is possible to measure the interfacial tension directly in our apparatus by recording drop retraction after a shear deformation. However, after cessation of shearing the uncompatibilized drops were unstable, breaking into smaller droplets. This is similar to the observations of Yamane et al.[35] By using smaller deformations, we got stable recovery. We could fit our length retraction to the 2D Newtonian analysis of Tjahjadi et al.,[36] but it required values of Γ higher than those reported in the literature. Again a 3D viscoelastic, finite element analysis is needed.

The compatibilized drops were less prone to breakup and recovered more slowly. The reactive systems showed the slowest recovery. Stability of the platelet structure is also very important for creating barrier films since in processing drops will experience changing shear and extension rates as well as a recovery period until they are frozen by cooling below the glass or crystallization temperature.

For the PS23 and PS-NH_2 drops sheared in the PE-MA matrix we attempted to measure the equilibrium drop size. After shear was stopped and started several times, only small, short cylinders remained. What was remarkable is that both the reactive and nonreactive systems gave the same size cylinders, 7−8 μm in diameter. Sundararaj and Macosko[28] also found no difference in drop size between block copolymer compatibilized and uncompatibilized polymer blends at steady-state mixing in the dilute drop limit. Sondergaard and Lyngaae Jorgenson[37] used light scattering to measure the increase in aspect ratio of PS drops in PMMA with a start up of shearing. With 2% P(S-*b*-MMA) the maximum aspect ratio was twice that without block copolymer; however, both systems went to the same equilibrium aspect ratio. If block copolymer simply lowers interfacial tension, we expect that in all three of these studies the steady-state sizes of the drops with block copolymer would be smaller. This was not observed. However, if block copolymers reduce slip in the interface, this should also reduce the steady-state size.

Another possiblity is gradients in interfacial tension. In drops of small molecule liquids, surfactants are known to concentrate at the ends of a deforming drop, causing a gradient in surfactant concentration.[38,39] The same phenomenon seems even more likely when large block copolymers are in a deforming interface.

Conclusions

Polymer drop deformation was observed using a parallel plate device with counterrotating transparent plates. The influence of block copolymers (BCPs) and in situ formed graft copolymers on polymer drop deformation was studied. It was found that interface modification had a pronounced effect on the amount of area generated during simple shear. The area which a minor phase creates during processing of polymer blends is the key for good barrier properties. The efficiency of stretching is measured in terms of reduced area, which is the ratio of the projected area to the cross-section of the initial drop. These measurements were compared to ideal affine and affine cylinder area generation.

Addition of 10% P(S-*b*-EE) block copolymer to two grades of polypropylene (melt index 2 and 30) resulted in a 2-fold increase in A_r^{max} for PP2 and 4-fold for PP30. BCP broadens the maximum of A_r and extends it to longer times, which is important if the morphology has to be preserved. Widening of the drop due to the much larger elasticity of the PS matrix compared to the PP30 drop results in greater than affine deformation. Significant effects were also found for the PMMA/PS pair with P(S-*b*-MMA) BCP. A small compatibilized drop (32 μm) generated 50% more reduced area than a larger drop (60 μm) without BCP.

Reactive PMMA-NH2 exhibits affine deformation even at high strain $\gamma > 40$ when sheared in PS-MA matrix. It gave nearly a 5-fold improvement in area generation over the nonreactive PMMA/PS-MA pair, although interfacial tension was relatively small, $\Gamma =$ 1.5 mN/m. Deformation of several different size drops of reactive polystyrene with end-functional amine groups was compared to similar size drops of nonreactive PS. Twice as much area was obtained at the maximum A_r for a 40 μm PS-NH_2 drop. A cross-linked "shell" around a PP-MA drop sheared in PS-OX matrix prevented the drop from deforming.

The greater deformability of drops with interfaces modified by block or graft copolymer may be due to reduction in interfacial tension or reduction in interfacial slip, but is probably a combination of these as well as tension gradients. Measurements and analysis of recovery after drop deformation may help to resolve this question and are also important for predicting final morphology in laminar blends for barrier films.

Acknowledgment. This work was supported by the National Science Foundation sponsored Center for Interfacial Engineering and grants from DuPont and the 3M Co. We wish to thank Frank Bates for providing us with the P(S-*b*-EE) block copolymer, Mark Gehlsen for the P(S-*b*-E) sample, John DeSimone for the PS−NH_2, and Russell Hooper and David Morse for helpful discussions.

References and Notes

(1) Subramanian, P. M. U.S. Patent 4,444,817, 1984; *Polym. Eng. Sci.* **1985**, *25*, 483.
(2) Taylor, G. I. *Proc. R. Soc., London* **1932**, *A138*, 41; **1934**, *A146*, 501.
(3) Grace, H. P. *Chem. Eng. Commun.* **1982**, *14*, 225.
(4) Bentley, B. J.; Leal, L. G. *J. Fluid Mech.* **1986**, *167*, 241.
(5) Rallison, J. M. *Annu. Rev. Fluid Mech.* **1984**, *16*, 45.
(6) Stone, H. A. *Annu. Rev. Fluid Mech.* **1994**, *26*, 65.
(7) Levitt, L.; Macosko, C. W.; Pearson, S. D. *Polym. Eng. Sci.* **1996**, *36*, 1647.
(8) Bates, F. S.; Kumar, A.; Schulz, M. *J. Polym. Sci., Part B: Polym. Phys.* **1995**, *33*, 1746. Weimann, P. A.; Jones, T. D.; Hillmyer, M. A.; Bates, F. S.; Londono, J. D.; Melnichenko, Y.; Wignall, G. D.; Almdal, K. *Macromolecules* **1996**, *30*, 3650.
(9) Guegan, P.; Macosko, C. W.; Ishizone, T.; Hirao, A.; Nakahama, S. *Macromolecules* **1994**, *27*, 4993.
(10) Gehlsen, M. D. Ph.D. Thesis, University of Minnesota, Minneapolis, 1994.
(11) Creton, C.; Kramer, E. J.; Hadziioannou, G. *Macromolecules* **1991**, *24*, 1846.
(12) Fetters, L. J.; Lohse, D. J.; Richter, D.; Witten, T. A.; Zirkel, A. *Macromolecules* **1994**, *27*, 4639.

(13) Plazek, D. J.; Tan, V.; O'Rourke, V. M. *Rheol. Acta* **1974**, *13*, 367.
(14) Raju, V. R.; Rachapudy, H.; Graessley, W. W. *J. Polym. Eng., Polym. Phys. Ed.* **1979**, *17*, 1223.
(15) Peters, M. A.; Belu, A. M.; Linton, R. W.; Dupray, L.; Meye, T. J.; DeSimone, J. M. *J. Am. Chem. Soc.* **1995**, *112*, 3380. See also: *Polym. Prepr. (Am. Chem. Soc., Div. Polym. Chem.)* **1993**, *34*, 374.
(16) Orr, C. A.; Adedeji; A.; Hirao, A.; Bates, F. S.; Macosko, C. W. *Macromolecules* **1997**, *30*, 1243.
(17) Fowler, M. W.; Baker, W. E. *Polym. Eng. Sci.* **1988**, *28*, 1427.
(18) Liu, N. C.; Baker, W. E. *Adv. Polym. Technol.* **1992**, *11*, 249.
(19) Sundararaj, U.; Macosko, C. W.; Nakayama, A.; Inoue, T. *Polym. Eng. Sci.* **1995**, *35*, 100.
(20) Levitt, L. Area Generation in Two-Phase Polymer Melt Processing. Ph.D. Thesis, University of Minnesota, Minneapolis, 1997.
(21) Meijer, H. E. H.; Janssen, J. M. H. Mixing of Immiscible Liquids. In *Mixing and Compounding of Polymers*; Manas-Zloczower, I., Tadmor, Z., Eds.; Hanser Publishers: New York, 1994. See also Macosko, C. W. *Rheology: Principles, Measurements and Applications*; Wiley VCH: New York, 1994; p 36.
(22) Sundararaj, U.; Dori, Y.; Macosko, C. W. *Polymer* **1995**, *36*, 1957.
(23) Guido, S.; Villone, M. *J. Rheol.* **1998**, *42*, 395.
(24) Reduction in viscosity with as little as 2% BCP has been observed. Jones, T. D.; Bates, F. S.; Macosko, C. W. *Polym. Prepr.* (*Am. Chem. Soc., Div. Polym. Chem.*), **1999**, *40:2*, 1097.
(25) Wu, S. *Polymer* **1987**, *26*, 1855.
(26) Elemans, P. H. M.; Janssen, J. M. H.; Meijer, H. E. H. *J. Rheol.* **1990**, *34*, 1311.
(27) Elmendorp, J. J.; de Vos, G. *Polym. Eng. Sci.* **1986**, *26*, 415.
(28) Sundararaj, U.; Macosko, C. W. *Macromolecules* **1995**, *28*, 2647.
(29) Van Oene, H. J. *Colloid Interface Sci.* **1972**, *40*, 448.
(30) Anastasiadas, S. H.; Gancarz, L.; Koberstein, J. T. *Macromolecules* **1989**, *22*, 1449.
(31) Mekhilef, N.; Favis, B. D.; Carreau, P. J. *J. Polym. Sci., Part B: Polym. Phys.* **1997**, *35*, 293.
(32) Hooper, R. W.; Macosko, C. W.; Derby, J. J. FEM Modeling of Transient Viscoelastic Drop Deformation in Extensional Flow. *J. Non Newt. Fluid Mech.*, submitted for publication.
(33) De Gennes, P. G. *C. R. Acad Sci., Ser. II: Mec., Phys., Chim., Astron.* **1989**, *308*, 1401. Brochard, F.; de Gennes, P. G.; Troian, S. *C. R. Acad Sci., Ser. III:* **1990**, *310*, 1169.
(34) Goveas, J. L.; Fredrickson, G. H. *Eur. Phys. J. B.* **1998**, *2*, 79.
(35) Yamane, H.; Takahashi, M.; Hayashi, R.; Okamoto, R.; Kashihara, H.; Masuda, T. *J. Rheol.* **1998**, *42*, 567.
(36) Tjahjadi, M.; Ottino, J. M.; Stone, H. A. *AIChE J.* **1994**, *40*, 385.
(37) Songergaard, K.; Lyngaae-Jorgensen, J. *Rheo-Physics of Multiphase Polymer Systems*; Technomic: Lancaster, PA, 1993; p 475.
(38) De Bruijn, R. A. *Chem. Eng. Sci.* **1993**, *48*, 277.
(39) Li, X.-F.; Pozrikidis, C. *J. Fluid Mech.* **1997**, *341*, 165.
(40) Levitt, L.; Macosko, C. W.; Schweizer, T.; Meissner, J. *J. Rheol.* **1997**, *41*, 671.

MA9814999